

Metal–Pteridine Complexes Having Three-Dimensional Hydrogen-Bonded Networks

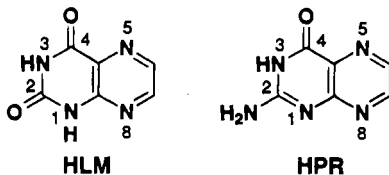
Minoru Mitsumi,^{1a} Jiro Toyoda,^{1b} and Kazuhiro Nakasuji^{*,1c}

Department of Functional Molecular Science, The Graduate University for Advanced Studies, Myodaiji, Okazaki 444, Japan, Institute for Molecular Science, Myodaiji, Okazaki 444, Japan, and Department of Chemistry, Faculty of Science, Osaka University, Toyonaka, Osaka 560, Japan

Received November 8, 1994

Introduction

Control of the cooperative interaction between electron transfer and proton transfer in hydrogen-bonded charge-transfer (HBCT) systems is a new way to regulate electronic properties in the solid state.^{2,3} In principle, CT interaction can be related to the redox properties of the metal atoms and/or the stacking interactions between the ligands. In order to study the basic chemistry of such systems, we need to construct metallosupramolecular systems in which a ligand is connected by intermolecular H-bonds. As a basic skeleton of the ligands, we have utilized the pteridine derivatives, such as lumazine (HLM) and pterin (HPR), which have the ability to chelate to metal atoms and H-bonding sites of NH \cdots O and NH \cdots N types in the solid state.



Pteridine–metal complexes have recently been studied to mimic both the metal environment and reactivity of the metal site of the enzymes, and some of these have been characterized by X-ray crystallography.^{4,5} We now report the crystal structures of some metal complexes having three-dimensional H-bonded networks and stacking interactions based on pteridine ligands, [Cu(LM)₂(H₂O)₂] (**1**), [Cu(PR)₂(H₂O)₂] (**2**), and [Zn(PR)₂(H₂O)₂]·2H₂O (**3**).

Experimental Section

Preparation of [Cu(LM)₂(H₂O)₂] (1**), [Cu(PR)₂(H₂O)₂] (**2**), and [Zn(PR)₂(H₂O)₂]·2H₂O (**3**).** The desired complexes are expected to

- (1) (a) The Graduate University for Advanced Studies. (b) Institute for Molecular Science. (c) Osaka University.
- (2) Nakasuji, K.; Sugiura, K.; Kitagawa, T.; Toyoda, J.; Okamoto, H.; Okaniwa, K.; Mitani, T.; Yamamoto, H.; Murata, I.; Kawamoto, A.; Tanaka, J. *J. Am. Chem. Soc.* **1991**, *113*, 1862–1864.
- (3) Mitani, T.; Saito, G.; Urayama, H. *Phys. Rev. Lett.* **1988**, *60*, 2299–2302.
- (4) Metal–pteridine complexes characterized by X-ray analysis are as follows: (a) Burgmayer, S. J. N.; Stiefel, E. I. *J. Am. Chem. Soc.* **1986**, *108*, 8310–8311. (b) Burgmayer, S. J. N.; Stiefel, E. I. *Inorg. Chem.* **1988**, *27*, 4059–4065. (c) Perkinson, J.; Brodie, S.; Yoon, K.; Mosny, K.; Carroll, P. J.; Morgan, T. V.; Burgmayer, S. J. N. *Inorg. Chem.* **1991**, *30*, 719–727. (d) Kohzuma, T.; Masuda, H.; Yamauchi, O. *J. Am. Chem. Soc.* **1989**, *111*, 3431–3433. (e) Odani, A.; Masuda, H.; Inukai, K.; Yamauchi, O. *J. Am. Chem. Soc.* **1992**, *114*, 6294–6300. (f) Nasir, M. S.; Karlin, K. D.; Chen, Q.; Zubietta, J. *J. Am. Chem. Soc.* **1992**, *114*, 2264–2265.
- (5) Goodgame, M.; Schmidt, M. A. *Inorg. Chim. Acta* **1979**, *36*, 151–154.

Table 1. Crystallographic Data for [Cu(LM)₂(H₂O)₂] (**1**), [Cu(PR)₂(H₂O)₂] (**2**), and [Zn(PR)₂(H₂O)₂]·2H₂O (**3**)

	1	2	3
chem formula	C ₁₂ H ₁₀ CuN ₈ O ₆	C ₁₂ H ₁₂ CuN ₁₀ O ₄	C ₁₂ H ₁₆ N ₁₀ O ₆ Zn
fw	425.81	423.84	461.70
space group	P1	P2 ₁ /n	P1
a, Å	6.419(1)	7.176(2)	7.604(1)
b, Å	11.437(3)	13.177(3)	8.563(2)
c, Å	5.112(1)	8.124(2)	7.028(2)
α, deg	94.07(2)		108.69(2)
β, deg	107.07(2)	107.12(2)	96.22(2)
γ, deg	81.00(2)		77.02(1)
V, Å ³	354.2(2)	734.2(4)	422.1(2)
Z	1	2	1
ρ _{calc} , g·cm ⁻³	1.996	1.917	1.816
T, K	296	296	296
λ, Å	0.710 69	0.710 69	0.710 69
μ, cm ⁻¹	16.01	15.40	15.16
R ^a	0.030	0.032	0.038
R _w ^b	0.034	0.038	0.054

$$^a R = \sum ||F_o| - |F_c|| / \sum |F_o|. \quad ^b R_w = \{(\sum w(|F_o| - |F_c|)^2 / \sum w|F_o|^2)\}^{1/2}.$$

have low solubility due to multi-intermolecular H-bonding interactions, which prevent the formation of single crystals by recrystallization procedures. Therefore, in order to prepare single crystals of **1–3**, we utilized a diffusion procedure of the deprotonated ligands and metal source in water. The ligands HLM and HPR were synthesized according to literature methods.⁶ The synthesis of **1** is typical. Vivid green crystals of **1** were obtained at room temperature by diffusion in an H-shaped tube (ca. 12 mL) containing an aqueous solution of Cu(ClO₄)₂·6H₂O (0.050 mmol, 0.5 mL), an aqueous solution (0.5 mL) of HLM (0.10 mmol) and NaOH (0.11 mmol), and water (11 mL) (yield 28%): IR (KBr, cm⁻¹) 3109 (s), 3061 (m), 3037 (br), 2966 (m), 2909 (m), 2812 (m), 2720 (m), 1654 (s), 1608 (vs), 1569 (vs), 1540 (s), 1510 (s), 1458 (m), 1417(s), 1395(s), 1312(s), 1296 (s), 1233(s), 1210 (m), 1166 (m), 1070 (m) 824 (m); UV/vis [in solid state (KBr pellet), λ_{max}, nm] 247, 355, 372, 438 (sh), 641 (br). Anal. Calcd for C₁₂H₁₀-CuN₈O₆: C, 33.85; H, 2.37; N, 26.32. Found: C, 33.45; H, 2.55; N, 26.29.

Single crystals of **2** and **3** were obtained by similar procedures. Diffusion condition for **2**: an aqueous solution (0.5 mL) of HPR (0.060 mmol) and NaOH (0.066 mmol), an aqueous solution of Cu(ClO₄)₂·6H₂O (0.030 mmol, 0.5 mL), and water (11 mL). Only a few deep yellowish green crystals of **2** were obtained from the powder deposited: IR (KBr, cm⁻¹) 3406 (s), 3310 (s), 3215 (s), 3116 (w), 1633 (s), 1603 (vs), 1548 (s), 1515 (m), 1466 (s), 1456 (s), 1391 (m), 1361 (s), 1335 (m), 1214 (m), 1171 (m), 1101 (m), 1077 (m), 828 (m); UV/vis [in solid state (KBr pellet), λ_{max}, nm] 265, 311 (sh), 388, 415 (sh), 620 (br).

Diffusion condition for **3**: an aqueous solution (0.5 mL) of HPR (0.075 mmol) and NaOH (0.083 mmol), an aqueous solution of Zn(NO₃)₂·6H₂O (0.038 mmol, 0.5 mL), and water (11 mL). Light greenish yellow crystals were obtained (yield 46%): IR (KBr, cm⁻¹) 3432 (s), 3400 (br), 3330 (br), 3297 (br), 3218 (sh), 3145 (s), 1636 (s), 1599 (vs), 1542 (s), 1525 (s), 1463 (s), 1390 (m), 1362 (s), 1332 (m), 1208 (s), 1110 (m), 1078 (m), 830 (m); UV/vis [in solid state (KBr pellet), λ_{max}, nm] 245 (sh), 268, 395, 420 (sh). Anal. Calcd for C₁₂H₁₆N₁₀O₆·Zn: C, 31.22; H, 3.49; N, 30.34. Found: C, 31.22; H, 3.43; N, 30.87.

Crystallographic Studies. Intensity data were collected at a temperature of 296 K on Rigaku AFC5R or AFC7R diffractometer with graphite-monochromated Mo Kα radiation and the ω–2θ scan technique. Accurate cell dimensions and crystal orientation matrices were determined by least-squares refinement of 25 (**1**), 18 (**2**), and 24 (**3**) reflections in the ranges 22.28 < 2θ < 29.67° (**1**), 20.62 < 2θ <

- (6) (a) For HLM (lumazine): Albert, A.; Brown, D. J.; Cheeseman, G. J. *Chem. Soc.* **1951**, 474–485. (b) For HPR (pterin): Mowat, J. H.; Boothe, J. H.; Hutchings, B. L.; Stokstad, E. L. R.; Waller, C. W.; Angier, R. B.; Semb, J.; Cosulich, D. B.; SubbaRow, Y. *J. Am. Chem. Soc.* **1948**, *70*, 14–18.

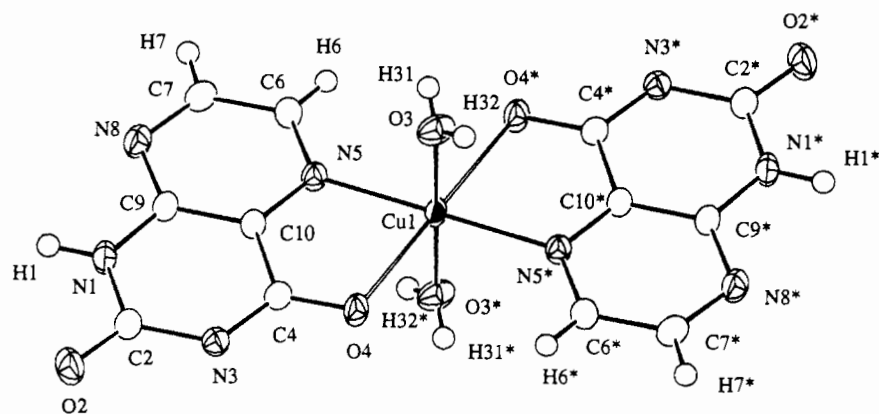


Figure 1. ORTEP diagram for **1** with atomic numbering scheme and 50% thermal ellipsoids. Selected bond lengths (Å) are as follows: Cu(1)–O(3), 1.975(2); Cu(1)–O(4), 2.329(2); Cu(1)–N(5), 2.022(2). Selected bond angles (deg) are as follows: O(3)–Cu(1)–O(4), 89.74(7); O(3)–Cu(1)–O(4'), 90.26(7); O(3)–Cu(1)–N(5), 89.00(7); O(3)–Cu(1)–N(5'), 91.00(7); O(4)–Cu(1)–N(5), 78.05(6); O(4)–Cu(1)–N(5'), 101.95(6).

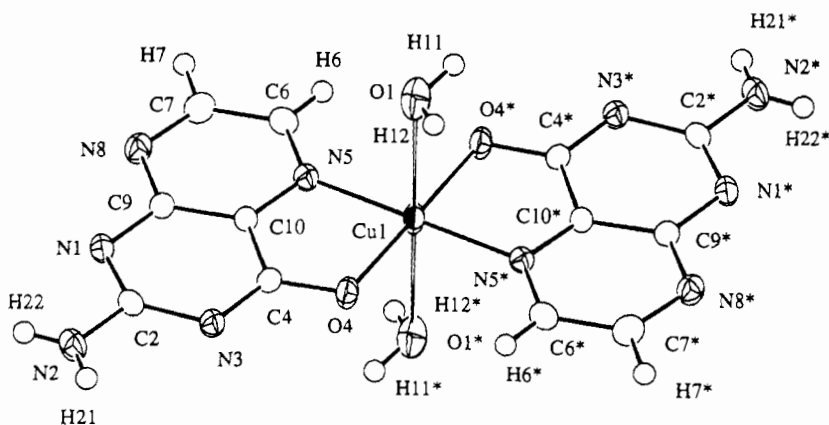


Figure 2. ORTEP diagram for **2** with atomic numbering scheme and 50% thermal ellipsoids. Selected bond lengths (Å) are as follows: Cu(1)–O(1), 2.586(3); Cu(1)–O(4), 1.985(2); Cu(1)–N(5), 1.976(2). Selected bond angles (deg) are as follows: O(1)–Cu(1)–O(4), 95.18(8); O(1)–Cu(1)–O(4'), 84.82(8); O(1)–Cu(1)–N(5), 88.58(8); O(1)–Cu(1)–N(5'), 91.42(8); O(4)–Cu(1)–N(5), 84.86(7); O(4)–Cu(1)–N(5'), 95.14(7).

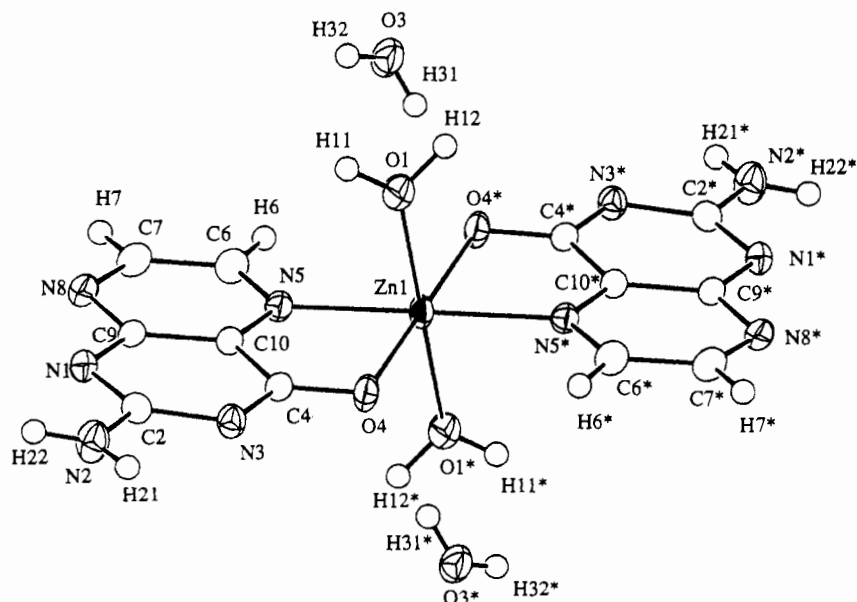


Figure 3. ORTEP diagram for **3** with atomic numbering scheme and 50% thermal ellipsoids. Selected bond lengths (Å) are as follows: Zn(1)–O(1), 2.169(2); Zn(1)–O(4), 2.059(2); Zn(1)–N(5), 2.162(2). Selected bond angles (deg) are as follows: O(1)–Zn(1)–O(4), 88.94(9); O(1)–Zn(1)–O(4'), 91.06(9); O(1)–Zn(1)–N(5), 88.46(9); O(1)–Zn(1)–N(5'), 91.54(9); O(4)–Zn(1)–N(5), 80.36(8); O(4)–Zn(1)–N(5'), 99.64(8).

36.65° (**2**), and 27.65 < 2 θ < 29.86° (**3**). The crystallographic data and structure refinement for **1–3** are summarized in Table 1. A more complete list of the crystallographic data is reported in Table S1 in the supplementary material.

Totals of 4118 (**1**), 2389 (**2**), and 2631 (**3**) reflections were collected to a maximum 2 θ value of 60.0°; 2059 (**1**), 2235 (**2**), and 2460 (**3**) of them were unique, and from these, 1747 (**1**), 1495 (**2**), and 2089 (**3**)

were assumed as observed ($I > 3\sigma(I)$). For all three structures the data were corrected for Lorentz, polarization, and absorption effects. No decay correction was applied.

The structures of **1–3** were solved by heavy-atom Patterson methods⁷ and expanded using Fourier techniques. All non-hydrogen atoms were refined anisotropically. Hydrogen atoms were located on a ΔF map and refined isotropically. The maximum and minimum peaks on the

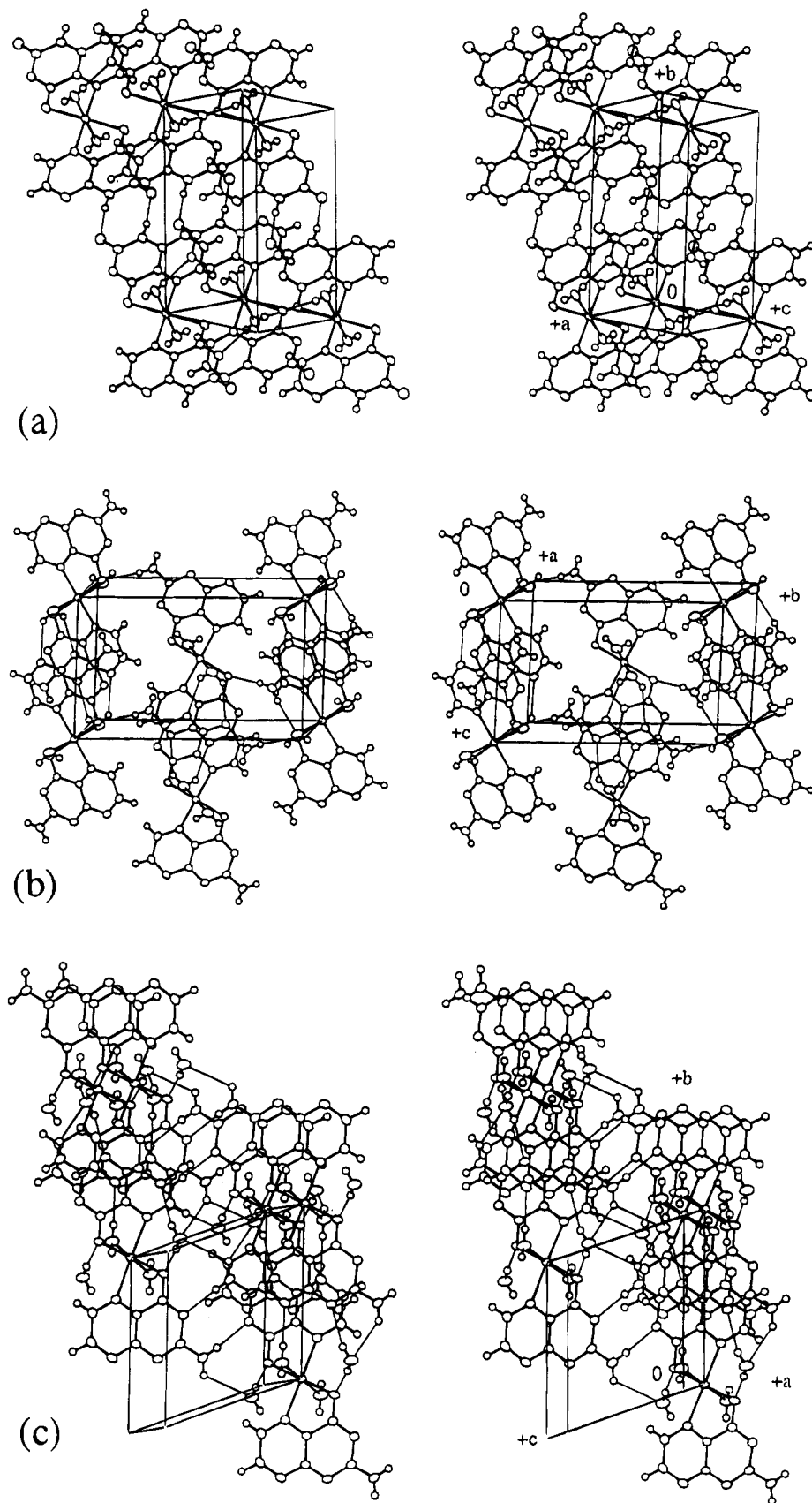


Figure 4. Stereoscopic ORTEP pairs of (a) $[\text{Cu}(\text{LM})_2(\text{H}_2\text{O})_2]$ (**1**), (b) $[\text{Cu}(\text{PR})_2(\text{H}_2\text{O})_2]$ (**2**), and (c) $[\text{Zn}(\text{PR})_2(\text{H}_2\text{O})_2] \cdot 2\text{H}_2\text{O}$ (**3**) showing the three-dimensional H-bonded network and pteridine stacking interactions.

final difference Fourier map corresponded to 0.36 and $-0.28 \text{ e } \text{\AA}^{-3}$ for **1**, 0.33 and $-0.32 \text{ e } \text{\AA}^{-3}$ for **2**, and 0.54 and $-0.76 \text{ e } \text{\AA}^{-3}$ for **3**, respectively. All calculations were performed using the teXsan⁸ crystallographic software package.

Results and Discussion

In the crystal structures, the three complexes possess an inversion center (Figure 1–3). In complex **1**, the copper(II)

Table 2. Hydrogen-Bonding Distances and Angles for [Cu(LM)₂(H₂O)₂] (1), [Cu(PR)₂(H₂O)₂] (2), and [Zn(PR)₂(H₂O)₂]·2H₂O (3)

D—H···A	D—H, Å	H···A, Å	D···A, Å	D—H···A, deg
[Cu(LM) ₂ (H ₂ O) ₂] (1)				
N(1)—H(1)···O(2) ^a	0.90(3)	1.96(3)	2.861(2)	173(3)
O(3)—H(31)···N(3) ^b	0.68(3)	2.03(3)	2.703(3)	168(3)
O(3)—H(32)···O(4) ^c	0.73(3)	1.96(3)	2.667(2)	164(3)
[Cu(PR) ₂ (H ₂ O) ₂] (2)				
N(2)—H(21)···O(4) ^d	0.83(3)	2.25(3)	3.068(3)	170(3)
N(2)—H(22)···O(1) ^e	0.80(3)	2.28(3)	3.076(3)	172(3)
O(1)—H(11)···N(8) ^f	0.88(5)	2.34(5)	3.055(3)	138(4)
O(1)—H(12)···N(1) ^g	0.75(4)	2.30(4)	2.896(3)	137(4)
[Zn(PR) ₂ (H ₂ O) ₂]·2H ₂ O (3)				
N(2)—H(21)···N(3) ^h	0.85(5)	2.18(5)	3.015(4)	169(4)
N(2)—H(22)···O(3) ⁱ	0.86(4)	2.34(4)	3.055(4)	141(4)
N(2)—H(22)···O(3) ^j	0.86(4)	2.63(4)	3.117(4)	117(3)
O(1)—H(11)···N(8) ^k	0.83(4)	2.07(4)	2.900(3)	173(4)
O(1)—H(12)···O(3) ^l	0.95(5)	1.83(5)	2.760(3)	166(4)
O(3)—H(31)···O(4) ^m	0.80(5)	2.03(5)	2.831(3)	175(4)
O(3)—H(32)···N(1) ⁿ	0.75(4)	2.11(5)	2.837(3)	162(5)

^{a–n} Symmetry operations: (a) 1 - x, 1 - y, -z; (b) -1 + x, y, z; (c) -x, -y, -1 - z; (d) 1/2 + x, -1/2 - y, 1/2 + z; (e) 1 - x, -y, 1 - z; (f) x, y, -1 + z; (g) x, y, -1 + z; (h) -1 - x, 1 - y, 1 - z; (i) -x, 1 - y, -z; (j) -1 + x, 1 + y, 1 + z; (k) -x, 1 - y, -z; (l) 1 - x, -y, -z; (m) -x, -y, -z; (n) -x, 1 - y, -z.

ion exhibits an elongated octahedral coordination. The basal plane consists of two N(5) atoms of LM ligands and two water molecules, and the two axial sites are occupied by two O(4) atoms of LM. In complex **2**, the coordination sphere of copper(II) ion has an elongated octahedral coordination geometry defined by two N(5) atoms and two O(4) atoms of PR ligands lying in the equatorial plane and by two water molecules at apices. In complex **3**, the zinc(II) ion is octahedrally surrounded by two water molecules and by two PR ligands bidentately coordinating through O(4) and N(5) atoms. The ZnN₂O₄ octahedron is markedly distorted. The Zn(II) ion deviates by 0.443 Å from the plane of the ligand PR, and the dihedral angle between the plane formed by O(4), Zn(1), and N(5) atoms and the ligand PR' plane is 15.29°.

Packing diagrams of the complexes **1–3** are presented in Figure 4. H-bonding distances and angles are given in Table 2.⁹ The molecular units of **1** are linked into a two-dimensional molecular sheet parallel to the *ac* plane via H-bonds between LM and coordinated water molecule (*a* direction, O(3)—H(31)···N(3)^b; *c* direction, O(3)—H(32)···O(4)^c). The molecular sheets are further linked to each other via double H-bonds between LM's (N(1)—H(1)···O(2)^a) in the [110] direction to form a three-dimensional H-bonded network. In the sheet, the pyrimidine and pyrazine rings of the LM ligands are stacked uniformly along the *c*-axis with a small overlap. The mean stacking distance is 3.27 Å.

The molecular units of **2** are linked into a two-dimensional molecular sheet parallel to the *ac* plane via H-bonds between PR and axial water molecule (*c* direction, O(1)—H(11)···N(8)^f and O(1)—H(12)···N(1)^g; [101] direction, N(2)—H(22)···O(1)^e). The molecular sheets are connected to each other via H-bonds

between the molecules related to the screw axis parallel to the *b*-axis, N(2)—H(21)···O(4)^d, to form a three-dimensional H-bonded network. There are two types of PR stacking along the *a*-axis with the alternated distances of 3.39 and 3.27 Å, respectively.

In **3**, the noncoordinated water molecules are involved in a three-dimensional H-bonded network. The molecular units are linked into a two-dimensional molecular sheet parallel to the *ab* plane via H-bonds between PR and coordinated water molecule (O(1)—H(11)···N(8)^k), between PR and noncoordinated water molecule (O(3)—H(31)···O(4)^m, O(3)—H(32)···N(1)ⁿ, and N(2)—H(22)···O(3)^j), and between coordinated and noncoordinated water molecules (O(1)—H(12)···O(3)^l). The molecular sheets are further linked to each other through double H-bonds of N(2)—H(21)···N(3)^h between molecular units related by a center of inversion in position [0.5, 0.5, 0.5] to form a three-dimensional H-bonded network. In addition, the hydrogen atom H(22) of the amino group is also involved in an intermolecular H-bond, N(2)—H(22)···O(3)^j, with the oxygen atom of uncoordinated water molecule, thus leading to a bifurcated H-bond around H(22). The structure contains two types of PR stacking along the *a*-axis with the alternated distances of 3.21 and 3.16 Å, respectively.

The IR spectra of the complexes **1–3** show substantial shifts to lower frequencies in the region 1750–1550 cm⁻¹ compared to the free ligands. Such shifts are nearly identical with the values reported,^{4c,5} and are typical of deprotonation of their neighboring protonated endocyclic nitrogens.

The correlation between O—H and N—H stretching frequencies and the corresponding interatomic distances of H-bonds, O···O, N···O, and N···N, has been reported.¹² Using this correlation, we can tentatively assign the absorption bands in the region 3600–2600 cm⁻¹. The estimated O—H and N—H stretching frequencies derived from the observed H-bonded distances are in good agreement with the major bands of the corresponding region (Tables S32 and S33 in the supplementary material). These correlations can be used to estimate H-bonding distances of structurally unknown compound.

In conclusion, the characteristic features in the crystal structures of the H-bonded metal complexes studied here are as follows: (1) the two pteridine ligands chelate to metal ion through the O(4) and N(5) donor atoms of pteridine; (2) the molecular units are connected to two-dimensional H-bonded molecular sheets by the coordinated water molecules; (3) in the molecular sheet, there are stacking structures of the pteridine skeleton; (4) the sheets are further connected to three-dimensional H-bonded networks via the H-bonded sites of the pteridine ligands; (5) almost all H-bonding sites existing in the molecule participate in intermolecular H-bonding interactions.

Acknowledgment. This work was partially supported by The Grant-in-Aid for Scientific Research from the Ministry of Education, Science, and Culture of Japan.

Supplementary Material Available: Tables giving crystal data and details of the structure determination, complete atom coordinates and *B* values, anisotropic thermal parameters, bond lengths and angles, and least-squares planes and ORTEP figures for compounds **1–3** (40 pages). Ordering information is given on any current masthead page.

- (7) (a) For **1** and **3**: Beurskens, P. T.; Admiraal, G.; Beurskens, G.; Bosman, W. P.; Garcia-Granda, S.; Gould, R. O.; Smits, J. M. M.; Smykalla, C. *PATY*, 1992. (b) For **2**: Fan, Hai-Fu. SAPI91. Structure Analysis Programs with Intelligent Control. Rigaku Corp., Tokyo, Japan, 1991.
- (8) teXsan. Crystal Structure Analysis Package. Molecular Structure Corp., the Woodlands, TX, 1985 and 1992.
- (9) We used the criterion for the existence of the H-bonding proposed by Hamilton and Ibers.¹⁰ The values for the atomic van der Waals radii are taken from the tabulation of Bondi.¹¹
- (10) Hamilton, W. C.; Ibers, J. A. *Hydrogen Bonding in Solids*; W. A. Benjamin: New York, 1968.
- (11) Bondi, A. J. *Phys. Chem.* **1964**, *68*, 441–451.

IC941289M

- (12) Nakamoto, I.^{3a} Novak,^{13b} and Lautié^{13c} have used graphical presentations to show the correlation between N—H and O—H stretching frequencies and the corresponding N···N, N···O, and O···O interatomic distances of H-bonded groups. Calculated D—H frequencies are extrapolated from the plots using the interatomic distances obtained from the crystallographic analysis.
- (13) (a) Nakamoto, K.; Margoshes, M.; Rundle, R. E. *J. Am. Chem. Soc.* **1955**, *77*, 6480–6486. (b) Novak, A. *Struct. Bonding (Berlin)* **1974**, *18*, 177–216. (c) Lautié, A.; Froment, F.; Novak, A. *Spectrosc. Lett.* **1976**, *9*, 289–299.